Dalton Transactions

PAPER

View Article Online
View Journal | View Issue

Cite this: *Dalton Trans.*, 2015, **44**, 13060

CFA-7: an interpenetrated metal–organic framework of the MFU-4 family†

Phillip Schmieder, Maciej Grzywa, Dmytro Denysenko, Manuel Hambach and Dirk Volkmer*

Received 4th May 2015,
Accepted 16th June 2015

DOI: 10.1039/c5dt01673h

www.rsc.org/dalton

The novel interpenetrated metal–organic framework **CFA-7** (Coordination Framework Augsburg University-7), $[Zn_5Cl_4(tqpt)_3]$, has been synthesized containing the organic linker {H_2-tqpt = 6,6,14,14-tetramethyl-6,14-dihydroquinoxalino[2,3-*b*]phenazinebistriazole}. Reaction of H_2-tqpt and anhydrous $ZnCl_2$ in *N*,*N*-dimethylformamide (DMF) yields **CFA-7** as pseudo-cubic crystals. **CFA-7** serves as precursor for the synthesis of isostructural frameworks with redox-active metal centers, which is demonstrated by postsynthetic metal exchange of Zn^{2+} by different M^{2+} (M = Co, Ni, Cu) ions. The novel framework is robust upon solvent removal and has been structurally characterized by single-crystal X-ray diffraction, TGA and IR spectroscopy, as well as gas sorption (Ar, CO_2 and H_2).

Introduction

The appearance of interpenetration in metal–organic frameworks (MOFs) has been described for a lot of MOFs in many articles.[1] The phenomenon has a great impact on the framework structure, and consequently also on potential functional properties of the resulting three-dimensional porous materials.[2]

Interpenetration, *i.e.* the occurrence of two or more structurally independent networks which are intergrown with each other, is a frequently observed phenomenon in MOF structural chemistry. The iconic MOF-5 was intensively investigated in terms of interpenetration in recent years.[3] Depending on water content, reaction time and temperature, molar ratio of metal salt-to-organic linker or the addition of agents like melamine, non-interpenetrated, partially or completely interpenetrated network variants of MOF-5 were obtained. Interpenetration in MOFs often leads to a reduced specific surface area of the network. On the other hand, interpenetrated frameworks may also feature some additional advantages such as improved network stability, increased heat of adsorption for certain molecular probes or enhanced molecular size selectivity.[3c,4]

Aiming to extend the range of isoreticular MFU-4-type frameworks, we here report on the synthesis and the structure of **CFA-7** (Coordination Framework Augsburg University-7) containing the largest straight linker molecule when compared to the organic bistriazolate linkers previously employed in the synthesis of porous MFU-4-type frameworks.[5–10]

The modular MFU-4 family is based on Kuratowski-type[11] pentanuclear secondary building units (SBUs) of the general formula $[M^{II}_5X_4(L_6)]$ (Fig. 1). In the pentanuclear coordination units, six triazolate ligands are monodentately coordinated to the central octahedrally coordinated Zn ion. The triazolate ligands are twisted around their coordinative bond to the central metal ion such that the nitrogen atoms are placed on the six edges of an imaginary tetrahedron, the four corners of which are occupied by four peripheral Zn ions. Accordingly, each of the latter are coordinated by three N donor atoms of the organic triazolate linkers. The coordination environment

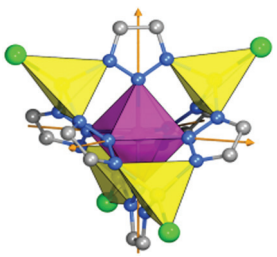

Fig. 1 Kuratowski-type SBU of MFU-4-type frameworks (central octahedrally coordinated metal ion: purple octahedron, peripheral Zn: yellow tetrahedra; N: blue; C: grey, Cl: green).

Institute of Physics, Chair of Solid State and Material Science, Augsburg University, Universitaetsstrasse 1, 86159 Augsburg, Germany.
E-mail: dirk.volkmer@physik.uni-augsburg.de; Fax: +49(0)821 598 5955; Tel: +49(0)821 598 3006

† Electronic supplementary information (ESI) available: XRPDs from **CFA-7** and its derivatives, NMR measurements of the organic linker, IR spectras and crystallographic data. CCDC 1062243. For ESI and crystallographic data in CIF or other electronic format see DOI: 10.1039/c5dt01673h

of each peripheral zinc ions is completed by an additional (anionic) ligand, *i.e.* a halide anion.

A special feature of the Kuratowski-type secondary building unit is the possibility to exchange the peripheral zinc ions by other (transition) metal ions. Adjusting appropriate reaction conditions it is possible to obtain heterometallic derivatives of **CFA-7** *via* postsynthetic metal exchange, as described previously for MFU-4l[7,9,10] and CFA-1.[8] Heating up **CFA-7** with solutions of the corresponding metal salts in *N*,*N*-dimethylacetamide (DMAc) leads to replacement of peripheral Zn^{2+} by M^{2+} (M = Co, Ni, Cu) ions. Depending on the metal source and the initial stoichiometric ratio of metal ions in the suspension, different numbers of zinc centers can be replaced by M^{2+} ions. **CFA-7** includes the fourth bistriazolate linker used to build MFU-4-type frameworks and represents the first framework of this type which is interpenetrated. Employing very long organic linkers we were aiming at MFU-4XL, a hypothetical cubic framework structure with extraordinary high specific surface area. The non-interpenetrated 3D structure of **CFA-7** is termed MFU-4extra large (MFU-4XL, calc. surface[17] up to 4500 $m^2\ g^{-1}$, Fig. 2 top right) due to its very large unit cell as compared to the previously published cubic networks of MFU-4[5] and MFU-4large[6] (Fig. 2). However, all attempts to synthesize the non-interpenetrated framework have failed in our hands so far.

Results and discussion

Syntheses and characterization

The H_2-tqpt ligand was synthesized in three steps. The 2,2,5,5-tetramethylcyclohexane-1,3-dione and the 3,3,6,6-tetramethylcyclohexane-1,2,4,5-tetraone were synthesized by conventional procedures.[12] The condensation reaction of the latter tetraone and two molecules of 1*H*-benzotriazole-5,6-diamine[13] leads to the organic triazolate linker H_2-tqpt (Scheme 1). The overall yield in these three steps is 21% based on dimedone as starting material. Metal–organic framework **CFA-7** can be synthesized from H_2-tqpt and $ZnCl_2$ in a good yield by using *N*,*N*-dimethylformamide (DMF) as solvent at 130 °C (see Scheme 2). At these reaction conditions the network forms light yellow pseudo-cubic crystals (Fig. 3a). A second, different morphology is obtained by adjusting a lower reaction temperature, *i.e.* at 90 °C. Under these conditions **CFA-7** crystals assume a hexagonal shape (Fig. 3b). Under reaction conditions identical to those in the synthesis of pseudo-cubic **CFA-7-chloride** (at 130 °C), employing ZnI_2 instead of $ZnCl_2$ however, pseudo-cubic yellow crystals of **CFA-7-iodide** were obtained. **CFA-7** and its iodide derivative **CFA-7-iodide** are isomorphous. A Le Bail fit[14] of the XRPD pattern of the compound **CFA-7-iodide** is presented in Fig. S1.† The refined unit cell parameters are: a = 28.6916(9) Å, c = 69.452(4) Å, V = 49 514(2) $Å^3$.

It is also possible to synthesize **CFA-7** in a microwave reactor at 250 W and 160 °C for 10 min. Morphology and surface details of the hexagonal crystals were investigated by DIC, SEM and AFM micrographs (Fig. 4–6). Differential interference contrast microscopy shows uniform hexagonal crystals with a size up to 30 μm (Fig. 4). Inspection of electron microscopic images reveals that the crystal faces of the hexagonal specimen are smooth and flat. An AFM measurement of a hexagonal single crystal of a size of about 30 × 30 μm was carried out in order to analyze the crystal's surface topography. In Fig. 6, it can be seen, that the surface is flat and exhibits no macroscopic height differences within the measured area.

Crystal structure analysis

Aiming to extend the range of isoreticular MFU-4-type frameworks, we calculated the hypothetical model for the cubic MFU-4extra large. The DFT calculated model (cell optimization employing plane-wave (norm-conserving) pseudo potentials, PBE functional, energy cut-off at 830 eV) of the structure is based on Kuratowski-type pentanuclear SBUs of the formula $[Zn_5Cl_4(tqpt)_3]$. Instead of the previously published cubic networks of MFU-4 or MFU-4large, respectively, the novel **CFA-7** network is twofold interpenetrated. Both subnetworks of **CFA-7** represent the same bond connectivity scheme as predicted for the hypothetical compound MFU-4XL. The previously reported MFU-4l has two different kinds of pores depending on the position of the four Cl-atoms from different Kuratowski SBUs. The A-and B-cells in MFU-4large have a diameter of 11.97 Å and 18.56 Å, respectively. The DFT calculated model of MFU-4XL shows pores with a diameter of 20.60 Å and 22.46 Å, respectively. The pore aperture in the non-interpenetrated framework is 11.94 Å.

A single-crystal X-ray diffraction study of a hexagonal crystal reveals that **CFA-7** crystallizes in the trigonal space group $R\bar{3}m$ (no. 166). *Pseudo-cubic* crystal of a size ranging from about 25–40 μm in each direction were also investigated but the single crystal structural analyses lead to the same solutions (trigonal crystal system and $R\bar{3}m$ space group), but the quality of the obtained data sets was lower in terms of resolution at high diffraction angles if compared to hexagonal crystal. The asymmetric unit including atom labels is presented in Fig. S15.† **CFA-7** is constructed from $\{Zn_5Cl_{4-x}((H_2O)_3)_x\}^{(6+x)+}$ secondary building units interconnected by the two-fold deprotonated organic linker $tqpt^{2-}$. Due to the conformationally flexible cyclohexyl unit in the middle of each organic linker molecule, the $tqpt^{2-}$ ligand in the **CFA-7** network is not completely planar. About 80% of the **CFA-7** network is constructed from regular $\{Zn_5Cl_4(triazolate)_6\}$ Kuratowski-type SBUs. The remaining 20% SBUs consist of singly charged $\{Zn_5Cl_3(H_2O)_3(triazolate)_6\}$ units, in which a single chloro ligand is replaced by 3 aqua ligands, thus leading to a non-coordinated (positionally strongly disordered) chloride anion which is placed in the void volume of the crystal lattice in order to retain a net zero charge. The zinc ions in the centers of the SBUs (Zn1 or Zn5, placed at a site of 3*m* symmetry) are octahedrally coordinated by six nitrogen atoms of six different organic linker molecules. The four peripheral zinc ions (Zn2 or Zn4, placed at sites of *m* symmetry) are four-fold coordinated by three nitrogen atoms of the organic linker and by the chloride anion. A fraction of 20% of the fourth peripheral zinc ions

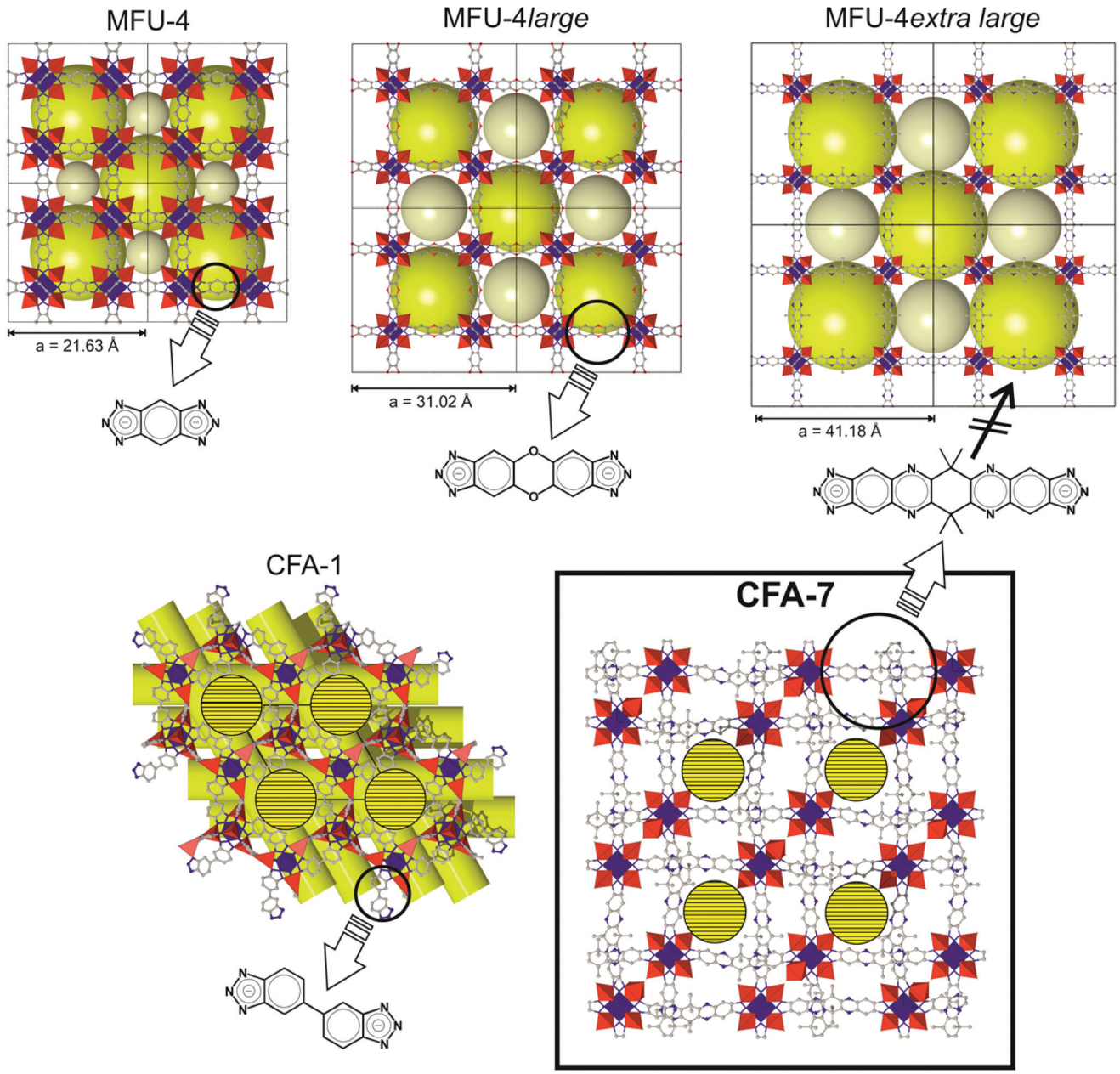

Fig. 2 An overview of different bistriazolate frameworks of the MFU-4 family with Kuratowski-type secondary building units. MFU-4, MFU-4l and the DFT-calculated MFU-4XL are representatives of the MFU-4 family which crystallize in a cubic crystal system, whereas CFA-1 exhibits a trigonal crystal lattice. The interpenetrated **CFA-7** framework described herein crystallizes in the trigonal space group $R\bar{3}m$ (no. 166).

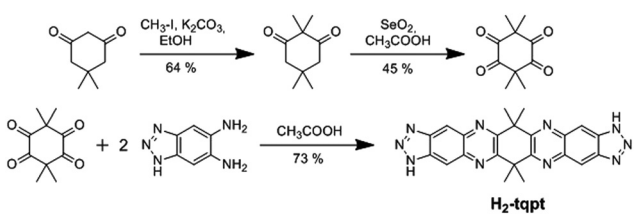

Scheme 1 Synthesis of the organic bistriazolate ligand H_2-tqpt.

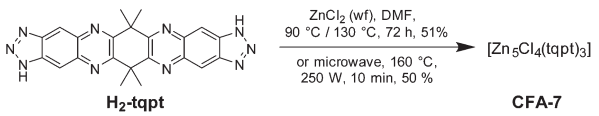

Scheme 2 Different synthesis procedures to obtain **CFA-7**.

(Zn3 or Zn6, positioned at a site of 3*m* symmetry) is octahedrally coordinated by three nitrogen atoms of the linker molecules and by three oxygen atoms from water molecules. The

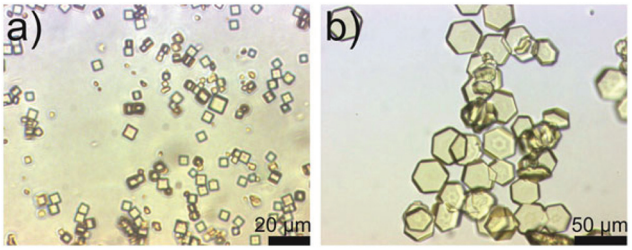

Fig. 3 Optical microscopy images of **CFA-7**: (a) overview of the as synthesized pseudo-cubic crystals; (b) hexagonal **CFA-7** crystals.

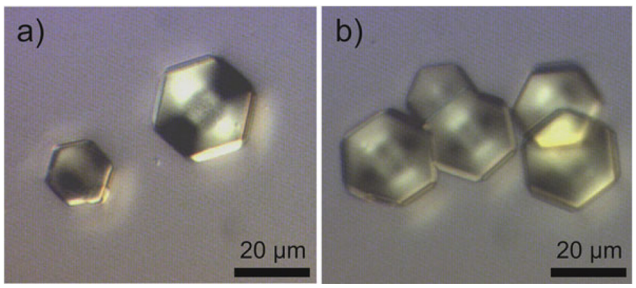

Fig. 4 Differential interference contrast (DIC) microscopy of hexagonal **CFA-7** crystals.

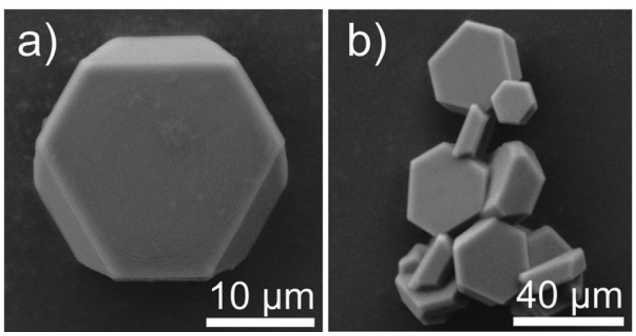

Fig. 5 SEM micrographs of **CFA-7**; (a) hexagonal shape of a single-crystal of **CFA-7**; (b) partially intergrown crystals.

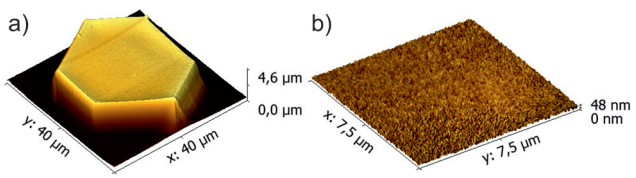

Fig. 6 AFM micrographs; (a) 3 dimensional view of a hexagonal **CFA-7** single crystal; (b) 3 dimensional view of **CFA-7** crystal surface.

different coordination schemes for both kinds of SBUs are shown in the plots in Fig. 8. The Zn–O distances are between 2.07–2.09 Å. These values are in good agreement with those found in the literature for similar Zn(II) compounds in which the octahedrally coordinated Zn ion binds three nitrogen containing ligands and three water molecules.[15] The Zn–N bond distances span a range of 2.150(10)–2.209(10) Å for the octahedrally coordinated Zn1 and Zn5 and 2.010(6)–2.135(13) Å for Zn2, Zn3, Zn4 and Zn6. These values are similar to those found in structurally related Zn triazolate compounds of the MFU-4 family.[10] **CFA-7** features a 3-D two-fold interpenetrated structure constructed from Kuratowski-type SBUs. The packing diagram of **CFA-7**, depicted in Fig. 7, shows two subnetworks. The simplified networks, displayed in red and blue colors, are shifted by 4.51 Å with respect to each other in [001] direction, which represents the shortest distance between two adjacent Zn ions belonging to different subnetworks). Fig. 7 also indicates the pseudo-cubic nature of the **CFA-7** network pointing at the close structural relation to the non-interpenetrated (hypothetical) MFU-4extra large network. Fig. 9 (left) shows a schematic representation of both subnetworks of **CFA-7**. The minimal divergence from right angles (Fig. 9 left) makes it impossible to solve the structure in a cubic space group.

Calculations with the program SQUEEZE[16] reveal that the initial solvent accessible void volume is 28 982 Å^3, which is about 58.3% of the unit cell volume (49 703 Å^3) for a probe radius of 1.68 Å, corresponding to the approximate van der Waals radius of argon.[17] In the crystal structure of **CFA-7** the pores are occupied by disordered Cl^- ions and DMF molecules. The positions of the molecules were impossible to resolve and to refine from the electron density distribution. According to the crystallographic data there is an electron count of 7108 per unit cell (rest of the electron density), which corresponds to approx. 5.34 Cl^- and 175 DMF molecules in the unit cell of **CFA-7**. Thus, the composition of the framework is determined

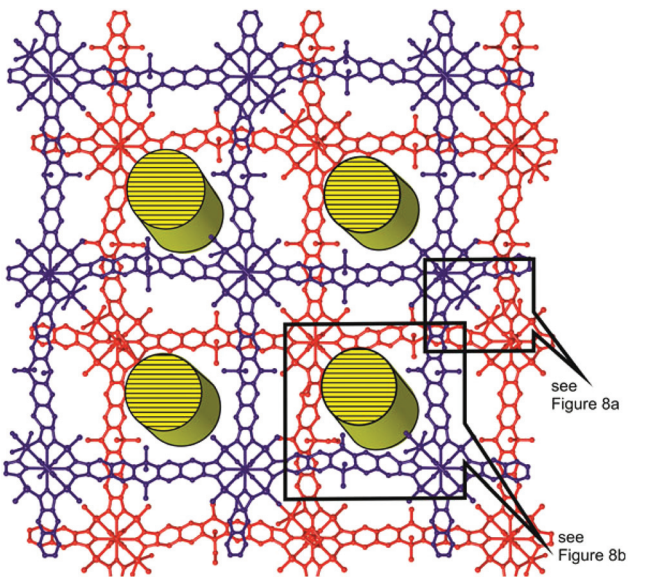

Fig. 7 Interpenetrated structure of **CFA-7**. In yellow the apparent pore aperture of the channels of the network is given (calculated with the Poreblazer software[17]).

as $[Zn_5Cl_{3.11}(H_2O)_{2.65}(tqpt)_3]^{(0.89+)}$ $(Cl^-)_{0.89}\cdot 29.25DMF$. This means, 0.89 chloride ions per SBU are displaced in the pores in order to retain neutral charge.

The calculation of maximal pore diameter and pore limiting diameter was performed using the Poreblazer software.[18] The limiting diameter in the **CFA-7** network is 6.83 Å and the maximum pore diameter is 11.71 Å. The diameter of the channels in the interpenetrated **CFA-7** network is 10.80 Å. The organic triazolate ligand of the network is disordered along the *c*-direction (Fig. 9 right). Three oxygen atoms of water ligands coordinating to Zn3 or Zn6 are placed in the interpenetrated frameworks in a way such that a staggered arrangement of the altogether six oxygen atoms of adjacent Kuratowski units is obtained (Fig. 8a). The non-bonding distances between two oxygen atoms of each SBU range from 2.87 Å to 4.16 Å. It is possible that hydrogen bridges are formed between the water ligands of the octahedrally coordinated zinc ions.

Up to now, it was not possible to synthesize the non-interpenetrated network of **CFA-7** (MFU-4extra large, Fig. 2). It is necessary to develop strategies to suppress the interpenetration in order to construct highly porous MOFs with high surface area. In literature different approaches for controlling the interpenetration in MOFs have been described.[3c,4] In our hands, varying the reaction temperature (in the range of 60–150 °C) and the concentration of the reaction mixture (in the range of 2–25 μmol ml^{-1}) had no influence on the interpenetration in **CFA-7**. Moreover, selecting solvents of different molecular size (*e.g. N*,*N*-dibutylformamide instead of DMF) did not lead to the synthesis of non-interpenetrated frameworks as confirmed by BET surface area measurements.

Thermal analysis and VTXRPD studies

The structural and thermal stability of **CFA-7** was investigated by TGA and VTXRPD measurements (Fig. 10 and 11). In the TGA curve of pre-dried (300 °C per vacuum, blue curve) **CFA-7** no weight loss in the range of 20–400 °C is observed. The as-synthesized sample of **CFA-7** shows a weight loss of 35%, which is due to the loss of DMF molecules. The decomposition of the framework under nitrogen flow starts at approx. 420 °C, which is in good agreement with VTXRPD data (Fig. 11).

Variable temperature X-ray powder diffraction studies (VTXRPD) show, similarly to the TGA data, that **CFA-7** is stable up to 400 °C in air.

Metal-exchange reactions

Heating up the framework with solutions of the corresponding metal salts in DMAc leads to replacement of peripheral Zn^{2+} by M^{2+} ions (M = Co, Ni, Cu). Depending on the stoichiometric ratio between metal salt and framework in the suspension, different fractions of zinc ions can be replaced by M^{2+} ions (Table 1). The octahedrally coordinated zinc centers in the centre of the SBUs cannot be replaced under the given experimental conditions, similar to experimental findings previously reported for MFU-4l[10] and CFA-1.[8] UV/Vis spectra of metal-exchanged **CFA-7** derivatives are shown in S 16. The spectro-

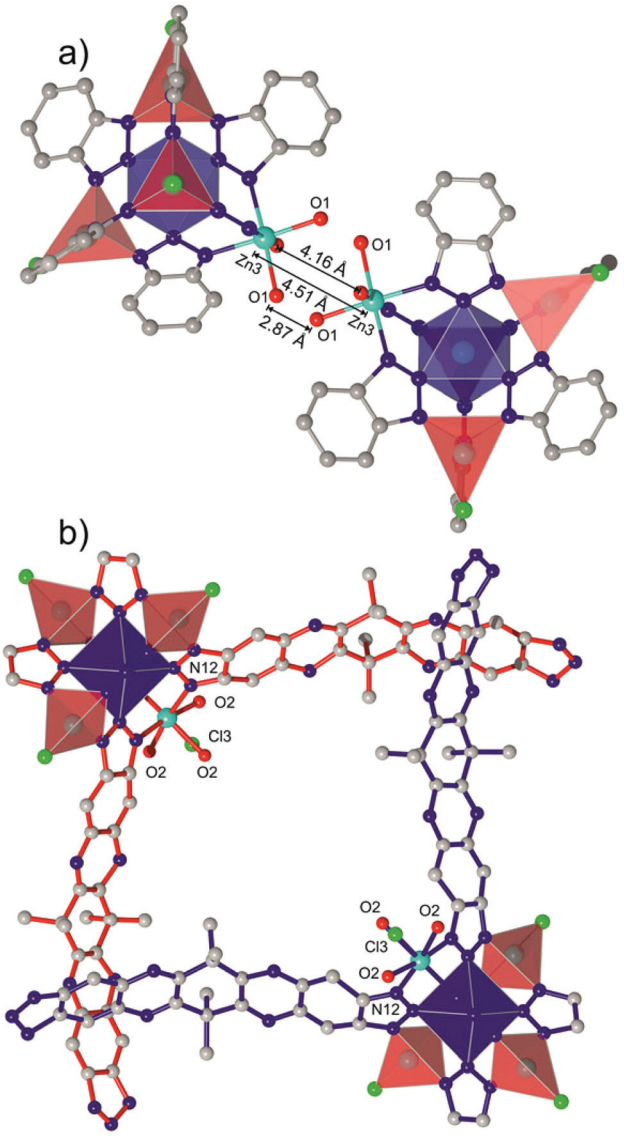

Fig. 8 Coordination environments of Zn ions in the Kuratowski-type secondary building units of **CFA-7**; (a) staggered arrangement of six water ligands from two different SBUs; (b) peripheral Zn ions which are coordinated to three N-atoms and one Cl-atom or to three N-atoms and three O-atoms.

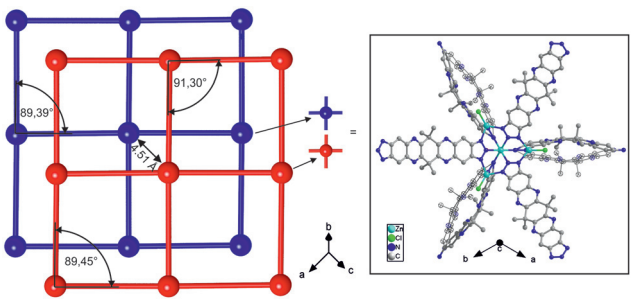

Fig. 9 Schematic representation of the two-fold interpenetrated **CFA-7** networks (left) and its SBU with the disordered organic linker in *c*-direction (right, positional disorder of two parts of the ligand with the occupancy of 0.5/0.5, one part shown in ellipses).

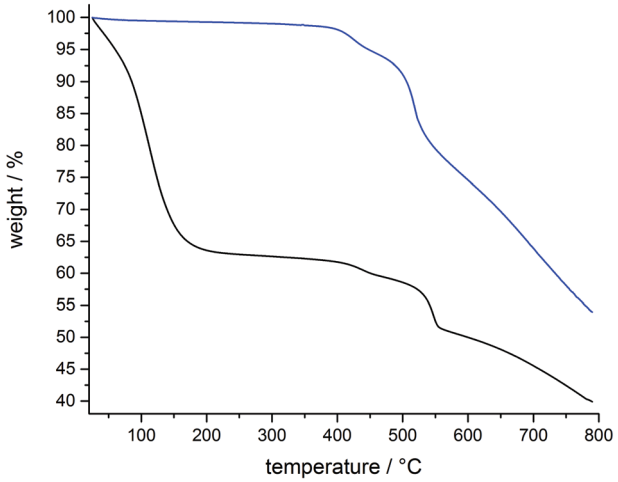

Fig. 10 Thermogravimetric analysis of pre-dried (blue) and not-dried (black) **CFA-7** under nitrogen atmosphere.

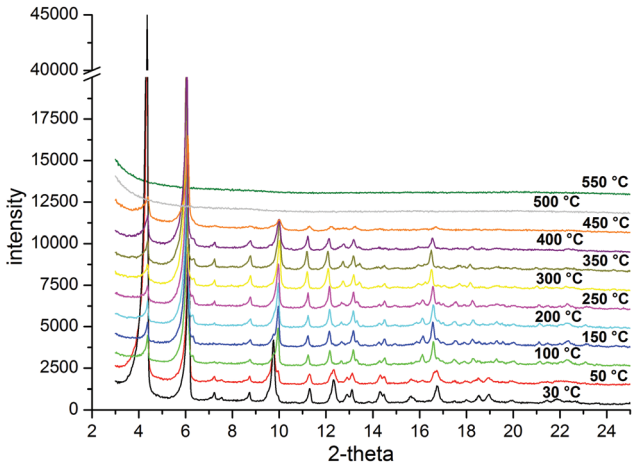

Fig. 11 VTXRPD plot of **CFA-7** in the range of 30–550 °C in air.

scopic measurements give no indication of octahedrally coordinated heterometallic ions. The diffuse reflectance UV/Vis spectra of **Co-CFA-7** shows strong absorption bands at *ca.* 600 nm, typical for Co(II) centers in tetrahedral coordination environments and correspond to the spin-allowed $^4A_2(F)$–$^4T_1(P)$ transition. The Mn-**CFA-7** shows no absorption bands in the UV/Vis spectrum relating to d–d metal-centered valence electron transitions. Copper(II)-exchanged derivatives show a weak band at *ca.* 950 nm. The position of the band maximum is in agreement with four coordinate tetrahedral Cu(II) complexes described in literature.[19,20] For **Co-CFA-7** the Le Bail fit of its X-ray powder pattern was performed in order to confirm that the structure of the framework remains intact. The refined unit cell parameters of **Co-CFA-7** are: a = 28.848(2) Å, c = 68.585(9) Å, V = 49 430(6) Å^3. The resulting plots are presented in Fig. S2.† The XRPD patterns of the other metal exchanged **CFA-7** samples, shown in Fig. S4,† also confirm the

Table 1 Overview of different metal exchange ratios obtained in reactions performed at T = 60 °C after 16 h

Metal salt	EDX [At%]	Molar ratio[a] Zn^{2+} : M^{2+}	Morphology	Color
$CuCl_2{\cdot}2H_2O$	Zn: 35.91 Cu: 23.72 Cl: 40.37	3.0 : 2.0	Cubes	Light brown
$Cu(ClO_4)_2{\cdot}6H_2O$	Zn: 19.70 Cu: 40.80 Cl: 39.50	1.6 : 3.4	Cubes	Brown
$CoCl_2{\cdot}6H_2O$	Zn: 38.35 Co: 20.55 Cl: 41.10	3.3 : 1.7	Cubes	Green
$NiCl_2$ (wf)	Zn: 36.16 Ni: 23.64 Cl: 40.20	3.0 : 2.0	Cubes	Dark yellow
$MnCl_2{\cdot}2H_2O$	Zn: 2.04 Mn: 94.01 Cl: 3.95	0.1 : 4.9	Cubes with contaminated surface	Dark brown

[a] Theoretical Zn^{2+} : M^{2+} ratio for total exchange of the peripheral metal atoms is 1 : 4.

stability of the framework upon metal exchange. In the case of manganese the Mn/Zn ratio obtained upon metal exchange is quite high, which is probably due to the precipitation of amorphous manganese impurities on the surface of the crystals (Fig. 12c). All exchange reactions were performed at 60 °C for 16 hours. The exchange reaction, when performed with copper(II) perchlorate gives a higher exchange ratio of peripheral zinc ions if compared to copper chloride employed as the source of metal ions. These transition metal containing frameworks are of potential interest for catalytic applications. The XRPD and IR data (Fig. S4 and S17†) of dry samples (300 °C per vacuum) indicate phase purity and thermal stability of all derivatives thus obtained.

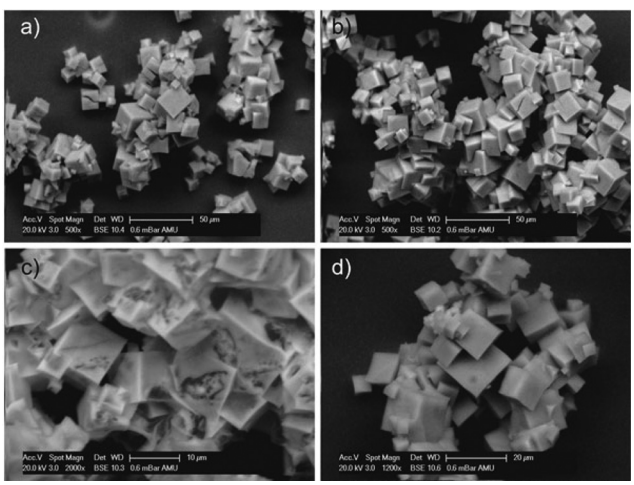

Fig. 12 SEM micrographs of **CFA-7**: (a) cubic **CFA-7** crystals after the postsynthetic metal exchange with $CoCl_2$; (b) exchange with $NiCl_2$; (c) metal exchange with $MnCl_2$; (d) crystals after exchange with $Cu(ClO_4)_2$.

Gas sorption measurements

The argon adsorption/desorption isotherm for **CFA-7** measured at 77.3 K follows type I behavior typical for microporous materials, no hysteresis is observed (Fig. S6†). Data analysis reveals the BET surface area of 1718 $m^2\ g^{-1}$ and Langmuir surface area of 1939 $m^2\ g^{-1}$ (calculated value with Poreblazer software: 1651 $m^2\ g^{-1}$). The total pore volume determined at p/p_0 = 0.99 is 0.70 $cm^3\ g^{-1}$, the micropore volume determined using an NLDFT method (pores up to 20 Å) is 0.61 $cm^3\ g^{-1}$ (calc. 0.66 $cm^3\ g^{-1}$). Porosity data for metal-exchanged **CFA-7** derivatives are given in ESI (Table S1 and Fig. S6†). Analysis using the non-local density functional theory (NLDFT) implementing a carbon equilibrium transition kernel for argon adsorption at 77 K based on a slit–pore mode[21] reveals quite broad distribution of micropores in the range of 5–16 Å with a maximum at 13.5 Å (Fig. 13). These values are in good agreement with the calculated values between 6.83–11.71 Å.

High-resolution CO_2 adsorption/desorption isotherms measured at 194.7 K show no hysteresis over the whole pressure range and thus confirm the structural rigidity of the interpenetrated **CFA-7** framework (Fig. 14).

The isosteric heat of CO_2 adsorption in **CFA-7** determined from the adsorption isotherms in the temperature range 273–293 K, as described in the ESI,† is nearly constant at 22.5 kJ mol^{-1} (Fig. 15). This value is considerably higher as the one determined previously for MFU-4l (16.5 kJ mol^{-1}),[22] which is most likely due to the presence of basic amino functions in the $tqpt^{2-}$ ligand. Alternatively, the increased heat of CO_2 adsorption could also be a special feature of the interpenetrated framework. However, the second explanation seems to be less likely since the heat of H_2 adsorption is very similar to MFU-4l and decreases constantly from 7.4 kJ mol^{-1} at 0.18 mmol g^{-1} loading to 6.2 kJ mol^{-1} at 2.2 mmol g^{-1} loading (Fig. 16).

Interpenetrated MOFs sometimes show flexible character due to displacement of individual sub-frameworks against

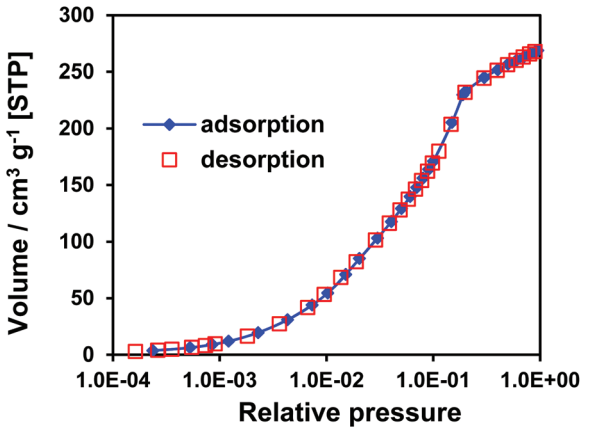

Fig. 14 CO_2 adsorption/desorption isotherm for **CFA-7** at 194.7 K.

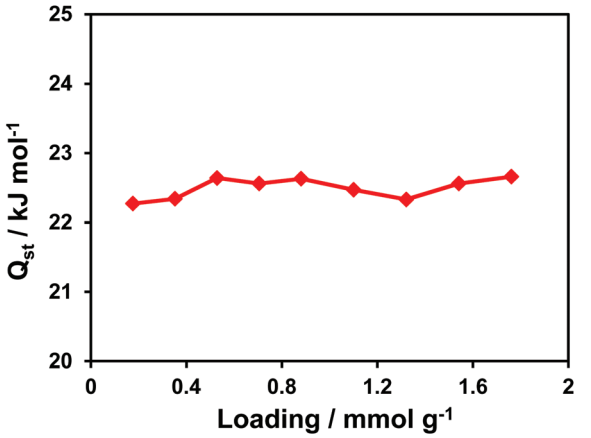

Fig. 15 Loading-dependent isosteric heat of CO_2 adsorption in **CFA-7**.

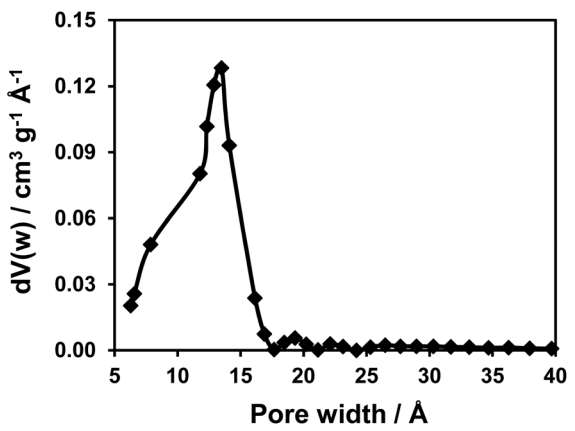

Fig. 13 Pore size distribution for **CFA-7** calculated by fitting NLDFT model to the Ar adsorption/desorption data.

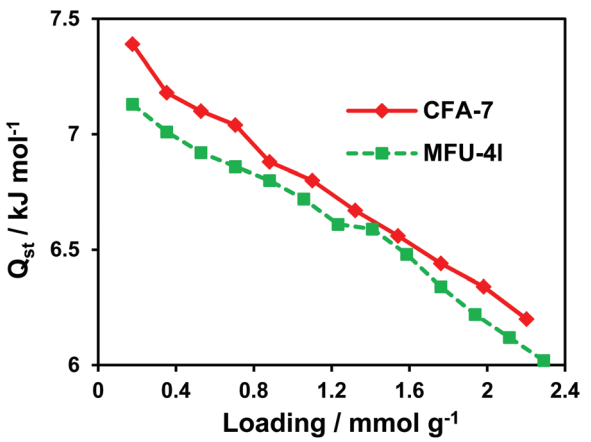

Fig. 16 Loading-dependent isosteric heats of H_2 adsorption in **CFA-7** and MFU-4l.

each other. Dramatic steps in the adsorption and hysteresis in the desorption of CO_2 have been observed in a twofold interpenetrated MOF, Zn2(bttb)(dpni) (bttb = 4,4,4,4-benzene-1,2,4,5-tetrayltetrabenzolate, dpni = *N*,*N*-di-(4-pyridyl)-1,4,5,8-naphthalenetetracarboxydiimide) reported by Hupp and co-workers.[23] Characterization of the structure by XRPD and pair distribution function (PDF) analysis indicated that structural changes upon CO2 sorption most likely involve the moving of the interpenetrated frameworks.[24]

In the interpenetrated **CFA-7** it seems as though the interpenetration has no direct influence on the sorption properties. The much higher heat of absorption from **CFA-7** for CO_2 compared to MFU-4l is mostly due to the interaction between the carbon dioxide and the additional nitrogen atoms with pyrazine character in the organic linker molecule. Based on theoretical considerations, the incorporation of accessible nitrogen-donor functional groups, such as pyridine, pyrazine, imidazole, and tetrazole, into the pore walls of porous materials can dramatically affect the gas uptake capacity and selectivity of the materials, especially for CO_2 capture, which most likely accounts for dipole–quadrupole interactions between the polarizable CO_2 molecule and the accessible nitrogen site.[25–31]

Conclusion

In conclusion, we have synthesized and structurally characterized a novel metal–organic framework (**CFA-7**) constructed from $tqpt^{2-}$ ligands and $\{Zn_5Cl_4\}^{6+}$ coordination units. This novel MOF contains Kuratowski-type pentanuclear SBUs, a characteristic feature of MFU-4-type frameworks. The **CFA-7** network is two-fold interpenetrated and thus the first example of an interpenetrated network of the MFU-4 family. The isolated subnetworks of the interpenetrated **CFA-7** show clearly the similarity with the cubic MFU-4, MFU-4large and the DFT-calculated hypothetical MFU-4extra large networks. Compared to the DFT-calculated MFU-4extra large model (calc. surface is 4460 $m^2\ g^{-1}$, limiting diameter is 11.91 Å and the maximum pore diameter is 22.46 Å) the interpenetrated **CFA-7** network shows much smaller values (BET surface area is 1718 $m^2\ g^{-1}$, limiting pore diameter is 6.83 Å and the maximum pore diameter is 11.71 Å). To compare the thermal stability of the network and the results from gas sorption measurements it is needful to synthesize the non-interpenetrated **CFA-7**.

A special feature of the system is the extended organic linker molecule with four additional (pyrazine) nitrogen atoms per linker molecule, which do not coordinate any metal ions under the reaction conditions described in this article. However, it might be possible to functionalize these N-donor sites under suitable reaction conditions, employing various organometallic reagents, for instance.

Similarly to MFU-4large and CFA-1 frameworks it is possible to exchange the peripheral Zn ions of each Kuratowski unit by Co(II), Cu(II) or Ni(II) to form open-shell 3d transition metal **CFA-7** derivatives as a versatile approach towards redox-active MOFs. Further attempts to synthesize the non-interpenetrated **CFA-7** framework ("MFU-4XL") are currently underway. Studying this framework would help to understand the nature of the increased isosteric heat of CO_2 adsorption which could also be a special feature of the interpenetrated framework.

Experimental section

Materials and methods

All starting materials were of reagent grade and used as received from the commercial supplier. Thermogravimetric analysis (TGA) was performed with a TGA Q500 analyzer in the temperature range of 25–800 °C in flowing nitrogen at a heating rate of 10 K min^{-1}. Argon gas sorption isotherms at 77.3 K in the range of $1.0 \times 10^{-5} \leq p/p_0 \leq 0.99$ were measured with a Quantachrome Autosorb-I ASI-CP-8 instrument. CO_2 and H_2 sorption isotherms were measured with a BELSORP-max instrument combined with a BELCryo system. Adsorbed gas amounts are given in $cm^3\ g^{-1}$ [STP], where STP = 101.3 kPa and 273.15 K. Prior to measurements, the sample was heated at 260 °C for 20 h in high vacuum in order to remove occluded solvent molecules. Fourier transform infrared (FTIR) spectra were recorded with ATR in the range 4000–180 cm^{-1} on a Bruker Equinox 55 FT-IR spectrometer. Energy-dispersive X-ray spectroscopy (EDX) was performed with a Philips XL 30 FEG scanning electron microscope equipped with an EDAX SiLi detector. Atomic force micrographs were recorded on an Agilent 5500 AFM with MAC III controller operating in tapping mode. Olympus AC160TS cantilevers with a force constant of 26 N m^{-1} (tip radius 9 ± 2 nm) were used at a resonance frequency of about 300 kHz.

The H_2-tqpt ligand was synthesized in three steps from commercially available 5,5-dimethylcyclohexane-1,3-dione.[11] The following methylation and oxidation reactions are documented in literature.[11] The 1*H*-benzotriazole-5,6-diamine was synthesized as described in literature.[12]

Synthesis of 6,6,14,14-tetramethyl-6,14-dihydroquinoxalino-[2,3-*b*]phenazinebistriazole, (H_2-tqpt)

To a suspension of 3,3,6,6-tetramethylcyclohexane-1,2,4,5-tetraone (1.00 g, 5.10 mmol) in CH_3COOH (200 mL), 1*H*-benzotriazole-5,6-diamine (1.60 g, 10.70 mmol) was added under good stirring. The suspension was heated to reflux for 24 hours. The dark red solution was cooled with an ice bath and diluted with 400 mL of water to precipitate a light yellow solid. The formed precipitate was filtered off and washed with H_2O and a small amount of MeOH.

Yield: 2.15 g (73%). ^{1}H NMR (400 MHz, DMSO-d_6/TFA-d, δ (ppm)): 11.67 (s, 4H, NH), 8.64 (s, 4H, ArH), 2.01 (s, 12H, $-CH_3$). ^{13}C NMR (100 MHz, DMSO-d_6/TFA-d, δ (ppm)): 156.65, 139.88, 138.47, 112.52, 45.83, 31.23. IR (ν (cm^{-1})): 1459.53, 1225.48, 1097.79, 850.99, 611.90, 412.05. Elemental analysis calcd for $C_{22}H_{18}N_{10}$ (%): C 62.55, H 4.29, N 33.16; found: C 62.58, H 4.20, N 33.22.

Synthesis of CFA-7

Heating block. A mixture of zinc chloride (10.8 mg, 0.08 mmol) and H_2-tqpt (10 mg, 0.02 mmol) was dissolved in 4 mL of *N*,*N*-dimethylformamide (DMF) and the solution was placed in a glass tube (10 mL). The tube was sealed and heated at 130 °C for 3 days and then cooled to room temperature. The precipitate was filtered, washed with DMF (3 × 1 mL) and MeOH (3 × 3 mL) and dried at 300 °C under vacuum.

Yield: 17.65 mg (51%). IR (ν (cm^{-1})): 1456, 1271, 1211, 1146, 1105, 1070, 850, 613, 310. Elemental analysis calcd (%) for $C_{66}H_{48}Cl_4N_{30}Zn_5$: C 45.82, H 2.80, N 24.29; found: C 45.89, H 2.71, N 24.30.

Microwave irradiation method. A mixture of zinc chloride (21.6 mg, 0.16 mmol) and H_2-tqpt (20 mg, 0.04 mmol) was dissolved in 1 mL of DMF and the solution was placed in a Pyrex sample tube (10 mL). The tube was sealed and placed in a microwave synthesizer (CEM, Discover S). The mixture was heated to 160 °C for 10 minutes at 250 W and then cooled to room temperature. The precipitate was filtered, washed with DMF (3 × 1 mL) and MeOH (3 × 3 mL) and dried at 300 °C under vacuum.

Synthesis of CFA-7-iodide derivative

A mixture of zinc iodide (25.6 mg, 0.08 mmol) and H_2-tqpt (10 mg, 0.02 mmol) was dissolved in 4 mL of DMF and the solution was placed in a glass tube (10 mL). The tube was sealed and heated at 140 °C for 3 days and then cooled to room temperature. The precipitate was filtered, washed with DMF (3 × 1 mL) and MeOH (3 × 3 mL) and dried at 300 °C under vacuum.

Yield: 20.11 mg (48%). IR (ν (cm^{-1})): 1410, 1311, 1196, 866, 422, 230. Elemental analysis calcd (%) for $C_{66}H_{48}I_4N_{30}Zn_5$: C 37.82, H 2.31, N 20.05; found: C 37.89, H 2.41, N 20.30.

General procedure for metal exchange reactions

The corresponding metal(II) salt (0.80 mmol) was dissolved in *N*,*N*-dimethylacetamide (DMAc) (4 mL) and activated **CFA-7** (5 mg, 0.003 mmol) was added to the solution. The suspension was heated for 16 hours at 60 °C in a sealed tube.

The particles were filtrated and washed several times with DMAc, methanol and dichloromethane. The sample was dried at 300 °C under vacuum.

Yield: 4.23–4.90 mg (90–97%); the number of M^{2+} ions in the formula unit calculated from the M^{2+}/Zn ratio was determined by EDX. All metal exchange reactions can be carried out in the same procedure with the corresponding metal salt. UV/vis and IR spectra are displayed in the ESI.†

Single-crystal X-ray diffraction

Several crystals of **CFA-7** were taken from mother liquids, mounted on a MiTeGen MicroMounts and tested on a diffractometer. Unfortunately, most of the crystals scattered only up to 40–42° θ (1.05–1.0 Å resolution). The best recorded data were obtained for a hexagonal single crystal of **CFA-7** of approx. dimensions 44 × 39 × 36 μm^3. The X-ray data for the single crystal structure determination of **CFA-7** were collected on a Bruker D8 Venture diffractometer. Intensity measurements were performed using monochromated (doubly curved silicon crystal) MoKα radiation (0.71073 Å) from a sealed microfocus tube. Generator settings were 50 kV, 1 mA. Data collection temperature was −173 °C. APEX2 software was used for preliminary determination of the unit cell.[32] Determination of integrated intensities and unit cell refinement were performed using SAINT.[33] The structure was solved and refined using the Bruker SHELXTL Software Package.[34] Selected crystal data and details of structure refinements for **CFA-7** are provided in Table 2. Complete crystallographic data for the structure $[Zn_5Cl_{3.11}(H_2O)_{2.65}(tqpt)_3]^{(0.89+)}$ $(Cl^-)_{0.89}$·29.25DMF reported in this paper have been deposited in the CIF format with the Cambridge Crystallographic Data Center, 12 Union Road, Cambridge CB21EZ, UK as supplementary publication no. CCDC 1062243.

(VT-)X-ray powder diffraction

VT-XRPD measurements were collected using a Bruker D8 Advance θ–2θ diffractometer in transmittance Bragg–Brentano geometry employing a Göbel mirror, Cu-radiation and equipped with a LYNXEYE 1-D detector. The samples were ground in an agate mortar and loaded into quartz capillaries (Hilgenberg) with 0.5 mm diameter and 0.01 mm wall thick-

Table 2 Crystal and experimental data for **CFA-7**

	CFA-7; $[Zn_5Cl_{3.11}(H_2O)_{2.65}(tqpt)_3]^{(0.89+)}$ $(Cl^-)_{0.89}$·29.25DMF
Compound	
Empirical formula	$C_{307.5}H_{516.1}$ $Cl_8N_{118.5}O_{63.8}Zn_{10}$ $C_{66}H_{53.3}Cl_{3.11}N_{30}O_{2.65}Zn_5$,
Formula	$Cl_{0.89}$29.25 (C_3H_7NO)
M_r/g mol^{-1}	7831.59
T/K	100(2)
Wavelength/Å	0.71073
Crystal system	Trigonal
Space group	$R\bar{3}m$ (no. 166)
a/Å	28.764(4)
c/Å	69.369(9)
V/$Å^3$	49 703(12)
Z	6
D_c/g cm^{-3}	1.570
μ/mm^{-1}	0.873
F(000)	24 822
θ Range/°	2.18 to 25.06
Refls. collected	200 917
Refls. unique	10 406
Data/restraints/parameters	10 406/264/453
R(int)	0.1992
GooF	1.129
R_1 ($I > 2\sigma(I)$][a]	0.1299
wR_2 (all data)[b]	0.3676
Largest diff. peak and hole/$Å^{-3}$	1.855 and −1.798

[a] $R_1 = \sum||F_o| - |F_c||/\sum|F_o|$. [b] $wR_2 = \sum[w(F_o^2 - F_c^2)^2]/\sum[w(F_o^2)^2]^{1/2}$.

ness. The patterns were recorded in a temperature range of 30 to 550 °C, in the 3–60° 2θ range, with a step time of 1 s and a step width of 0.02° 2θ. Temperature program between measurements: 0.5 °C s^{-1} heating rate, followed by 10 min isothermal steps required for recording diffraction data sets. The Le Bail fits were performed using the Jana2006 program.[35]

Acknowledgements

Financial support by the DFG (Priority Program SPP 1362 "Porous Metal–organic Frameworks") is gratefully acknowledged.

Notes and references

1 (*a*) T. Reineke, M. Eddaoudi, D. Moler, M. O'Keeffe and O. Yaghi, *J. Am. Chem. Soc.*, 2000, **122**, 4843; (*b*) H.-L. Jiang, T. Makal and H.-C. Zhou, *Coord. Chem. Rev.*, 2013, **257**, 2232; (*c*) B. Chen, X. Wang, Q. Zhang, X. Xi, J. Cai, H. Qi, S. Shi, J. Wang, D. Yuan and M. Fang, *J. Mater. Chem.*, 2010, **20**, 3758; (*d*) H. Xu, W. Bao, Y. Xu, X. Liu, X. Shen and D. Zhu, *CrystEngComm*, 2012, **14**, 5720; (*e*) E. Procopio, N. Padial, N. Masciocchi, S. Galli, J. Oltra, E. Barea and J. A. R. Navarro, *CrystEngComm*, 2013, **15**, 9352.

2 (*a*) K. Mulfort, O. Farha, C. Malliakas, M. Kanatzidis and J. Hupp, *Chem. – Eur. J.*, 2010, **16**, 276; (*b*) K. Mulfort and J. Hupp, *J. Am. Chem. Soc.*, 2007, **129**, 9604; (*c*) S. Bureekaew, H. Sato, R. Matsuda, Y. Kubota, R. Hirose, J. Kim, K. Kato, M. Takata and S. Kitagawa, *Angew. Chem., Int. Ed.*, 2010, **49**, 7660.

3 (*a*) J. Hafizovis, M. Bjoergen, U. Olsbye, P. Dietzel, S. Borgida, C. Prestipino, C. Lamberti and K. P. Lillerud, *J. Am. Chem. Soc.*, 2007, **129**, 3612; (*b*) B. Chen, X. Wang, Q. Zhang, X. Xi, J. Cai, H. Qi, S. Shi, J. Wang, D. Yuan and M. Fang, *J. Mater. Chem.*, 2010, **20**, 3758; (*c*) H. Kim, S. Das, M. G. Kim, D. N. Dybtsev, Y. Kim and K. Kim, *Inorg. Chem.*, 2011, **50**, 3691.

4 (*a*) M. K. Maji, R. Matsuda and S. Kitagawa, *Nat. Mater.*, 2007, **6**, 142; (*b*) S. Ma, X.-S. Wang, D. Yuan and H.-C. Zhou, *Angew. Chem., Int. Ed.*, 2008, **47**, 4130; (*c*) B. Kesanli, Y. Cui, M. R. Smith, E. W. Bittner, B. C. Bockrath and W. Lin, *Angew. Chem., Int. Ed.*, 2005, **44**, 72.

5 S. Biswas, M. Grzywa, H. P. Nayek, S. Dehnen, I. Senkovska, S. Kaskel and D. Volkmer, *Dalton Trans.*, 2009, 6487.

6 D. Denysenko, M. Grzywa, M. Tonigold, B. Streppel, I. Krkljus, M. Hirscher, E. Mugnaioli, U. Kolb, J. Hanss and D. Volkmer, *Chem. – Eur. J.*, 2011, **17**, 1837.

7 D. Denysenko, T. Werner, M. Grzywa, A. Puls, V. Hagen, G. Eickerling, J. Jelic, K. Reuter and D. Volkmer, *Chem. Commun.*, 2012, **48**, 1236.

8 P. Schmieder, D. Denysenko, M. Grzywa, B. Baumgärtner, I. Senkovska, S. Kaskel, G. Sastre, L. v. Wüllen and D. Volkmer, *Dalton Trans.*, 2013, **42**, 10786.

9 D. Denysenko, M. Grzywa, J. Jelic, K. Reuter and D. Volkmer, *Angew. Chem., Int. Ed.*, 2014, **53**, 5832.

10 D. Denysenko, J. Jelic, K. Reuter and D. Volkmer, *Chem. – Eur. J.*, 2015, **21**, 8188.

11 (*a*) S. Biswas, M. Tonigold and D. Volkmer, *Z. Anorg. Allg. Chem.*, 2008, **634**, 2532; (*b*) S. Biswas, M. Tonigold, M. Speldrich, P. Kögerler, M. Weil and D. Volkmer, *Inorg. Chem.*, 2010, **49**, 7424; (*c*) Y.-Y. Liu, M. Grzywa, M. Tonigold, G. Sastre, T. Schüttrigkeit, N. S. Leeson and D. Volkmer, *Dalton Trans.*, 2011, **40**, 5926.

12 (*a*) Y. Gaoni and E. Wenkert, *J. Org. Chem.*, 1966, **31**, 3809; (*b*) G. M. Whitesides and W. J. Ehmann, *J. Org. Chem.*, 1970, **35**, 3565; (*c*) R. Gleiter, T. Doerner and H. Irngartinger, *Liebigs Ann.*, 1996, 381.

13 J. Liu, J. M. Balkovec, A. D. Krikorian, D. Guiadeen, G. Yang, T. Jian, Z. Wu, Y. Yu, R. P. Nargund and P. Vachal, *PCT Int. Appl*, WO 2012044567, 2012.

14 (*a*) A. Le Bail, *Mater. Res. Bull.*, 1988, **23**, 447; (*b*) A. Le Bail, *Powder Diffr.*, 2005, **20**, 316.

15 (*a*) V. Gomez, J. Benet-Buchholz, E. Martin and J. R. Galan-Mascaros, *Chem. – Eur. J.*, 2014, **20**, 5369; (*b*) D. Hutchinson, M. James and S. Moratti, *Inorg. Chem.*, 2014, **53**, 2122; (*c*) Z.-Q. Liu, W. Dong and S. W. Ng, *Acta Crystallogr., Sect. E: Struct. Rep. Online*, 2007, **63**, 2943.

16 A. L. Spek, *J. Appl. Crystallogr.*, 2003, **36**, 7.

17 *Quantachrome Autosorb, Version 1.56*, Quantachrome GmbH & Co. KG, Odelzhausen, Germany, 2009.

18 L. Sarkisov and A. Harrison, *Mol. Simul.*, 2011, **37**(14), 1248.

19 A. B. P. Lever, in *Inorganic Electronic Spectroscopy*, 1984, p. 570ff.

20 O. R. Rodig, T. Brueckner, B. K. Hurlburt, R. K. Schlatzer, T. L. Venable and E. Sinn, *J. Chem. Soc., Dalton Trans.*, 1981, 196.

21 J. Jagiello and M. Thommes, *Carbon*, 2004, **42**, 1227.

22 G. Sastre, J. van den Bergh, F. Kapteijn, D. Denysenko and D. Volkmer, *Dalton Trans.*, 2014, **43**, 9612–9619.

23 K. Mulfort, O. Farha, C. Malliakas, M. Kanatzidis and T. Hupp, *Chem. – Eur. J.*, 2010, **16**, 276.

24 J.-R. Li, Y. Ma, M. C. McCarthy, J. Sculley, J. Yu, H.-K. Jeong, P. Balbuena and H.-C. Zhou, *Coord. Chem. Rev.*, 2011, **255**, 1791.

25 X.-J. Wang, P.-Z. Li, Y. Chen, Q. Zhang, X. Chan, R. Ganguly, Y. Li, J. Jiang and Y. Zhao, *Sci. Rep.*, 2013, **3**, 1149.

26 R. Vaidhyanathan, S. Iremonger, G. Shimizu, P. Boyd, S. Alavi and T. Woo, *Science*, 2010, **330**, 650.

27 W. Li, H. Shi and J. Zhang, *ChemPhysChem*, 2014, **15**, 1772.

28 S. Couck, J. Denayer, G. Baron, T. Remy, J. Gascon and F. Kapteijn, *J. Am. Chem. Soc.*, 2009, **131**, 6326.

29 N. Du, H. Park, G. Robertson, M. Dal-Cin, T. Visser, L. Scoles and M. Guiver, *Nat. Mater.*, 2011, **10**, 372.
30 F. Wang, Y.-X. Tan, H. Yang, Y. Kang and J. Zhang, *Chem. Commun.*, 2012, **48**, 4842.
31 R. Vaidhyanathan, S. Iremonger, K. Dawson and G. Shimizu, *Chem. Commun.*, 2009, 5230.
32 *APEX2 Version 2011.6*, Bruker AXS Inc.
33 *SAINT Version 8.32B*, Bruker AXS Inc., 2013.
34 *XL Version 2013/3*; G. M. Sheldrick, *Acta Crystallogr., Sect. A: Fundam. Crystallogr.*, 2008, **64**, 112.
35 V. Petricek, M. Dusek and L. Palatinus, *Jana2006, Structure Determination Software Programs*, Institute of Physics, Praha, Czech Republic, 2006.